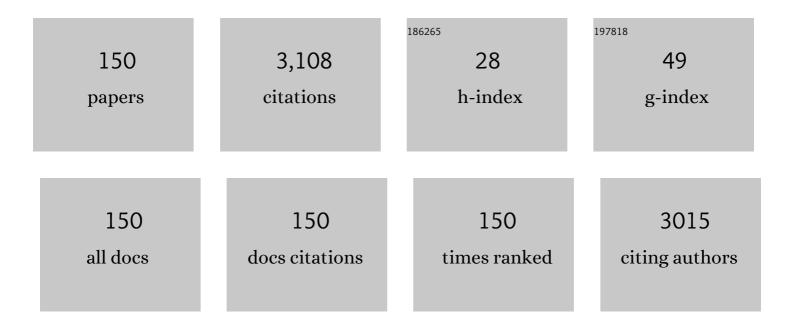
## Yutaka Majima

List of Publications by Year in descending order

Source: https://exaly.com/author-pdf/4841226/publications.pdf Version: 2024-02-01



ΥΠΤΑΚΑ ΜΑΠΜΑ

#	Article	IF	CITATIONS
1	Crystallization and electrical resistivity of Cu2O and CuO obtained by thermal oxidation of Cu thin films on SiO2/Si substrates. Thin Solid Films, 2012, 520, 6368-6374.	1.8	250
2	Generation of Maxwell displacement current from spread monolayers containing azobenzene. Journal of Applied Physics, 1992, 72, 1631-1636.	2.5	196
3	Generation of Maxwell displacement current across an azobenzene monolayer by photoisomerization. Nature, 1991, 353, 645-647.	27.8	130
4	Single Molecular Orientation Switching of an Endohedral Metallofullerene. Nano Letters, 2005, 5, 1057-1060.	9.1	128
5	Investigations of the dynamic behavior of fatty acid monolayers at the air–water interface using a displacement currentâ€measuring technique coupled with the Langmuirâ€film technique. Journal of Chemical Physics, 1991, 94, 5135-5142.	3.0	87
6	Robust nanogap electrodes by self-terminating electroless gold plating. Nanoscale, 2012, 4, 7161.	5.6	86
7	Nanoparticle characterization based on STM and STS. Chemical Society Reviews, 2015, 44, 970-987.	38.1	82
8	Logic Operations of Chemically Assembled Single-Electron Transistor. ACS Nano, 2012, 6, 2798-2803.	14.6	79
9	Simultaneous fabrication of nanogap gold electrodes by electroless gold plating using a common medical liquid. Applied Physics Letters, 2007, 91, 203107.	3.3	68
10	Gap separation-controlled nanogap electrodes by molecular ruler electroless gold plating. RSC Advances, 2015, 5, 22160-22167.	3.6	67
11	Tunneling resistance of double-barrier tunneling structures with an alkanethiol-protected Au nanoparticle. Physical Review B, 2005, 72, .	3.2	65
12	Characterization of Ni thin films following thermal oxidation in air. Journal of Vacuum Science and Technology B:Nanotechnology and Microelectronics, 2014, 32, .	1.2	65
13	Determination of the Dipole Moment of a Monolayer at the Air/Water Interface Using a Current-Measuring Technique. Japanese Journal of Applied Physics, 1988, 27, 721-725.	1.5	58
14	Single Electron on a Nanodot in a Double-Barrier Tunneling Structure Observed by Noncontact Atomic-Force Spectroscopy. Physical Review Letters, 2006, 96, 016108.	7.8	55
15	Scalability of carbon-nanotube-based thin film transistors for flexible electronic devices manufactured using an all roll-to-roll gravure printing system. Scientific Reports, 2015, 5, 14459.	3.3	54
16	Uniform charging energy of single-electron transistors by using size-controlled Au nanoparticles. Applied Physics Letters, 2012, 100, 033101.	3.3	52
17	Fully R2Râ€Printed Carbonâ€Nanotubeâ€Based Limitless Length of Flexible Activeâ€Matrix for Electrophoretic Display Application. Advanced Electronic Materials, 2020, 6, 1901431.	5.1	49
18	Enhancement of Ultrahigh Rate Chargeability by Interfacial Nanodot BaTiO <sub>3</sub> Treatment on LiCoO <sub>2</sub> Cathode Thin Film Batteries. Nano Letters, 2019, 19, 1688-1694.	9.1	47

#	Article	IF	CITATIONS
19	Crystallization and surface morphology of Au/SiO2 thin films following furnace and flame annealing. Surface Science, 2009, 603, 2978-2985.	1.9	46
20	Single-Electron Transistor Fabricated by Two Bottom-Up Processes of Electroless Au Plating and Chemisorption of Au Nanoparticle. Japanese Journal of Applied Physics, 2010, 49, 090206.	1.5	46
21	A new displacement current measuring system coupled with the Langmuirâ€film technique. Review of Scientific Instruments, 1991, 62, 2228-2233.	1.3	44
22	Bias Stress Induced Threshold Voltage Shift in Pentacene Thin-Film Transistors. Japanese Journal of Applied Physics, 2006, 45, L1127-L1129.	1.5	43
23	Fabrication and Characterization of Fully Flattened Carbon Nanotubes: A New Graphene Nanoribbon Analogue. Scientific Reports, 2013, 3, 1617.	3.3	39
24	Room-Temperature Coulomb Blockade from Chemically Synthesized Au Nanoparticles Stabilized by Acid–Base Interaction. Applied Physics Express, 2010, 3, 105003.	2.4	38
25	Proving Scalability of an Organic Semiconductor To Print a TFT-Active Matrix Using a Roll-to-Roll Gravure. ACS Omega, 2017, 2, 5766-5774.	3.5	38
26	Preparation of Oriented Langmuir-Blodgett Films of Polysilanes Bearing Hydroxyalkyl or Alkoxyalkyl Groups. Macromolecules, 1994, 27, 1911-1914.	4.8	37
27	Negative Differential Resistance by Molecular Resonant Tunneling between Neutral Tribenzosubporphine Anchored to a Au(111) Surface and Tribenzosubporphine Cation Adsorbed on to a Tungsten Tip. Journal of the American Chemical Society, 2013, 135, 14159-14166.	13.7	32
28	Investigation of photoinduced molecular switching in a single monolayer by a displacementâ€currentâ€measuring technique. Journal of Chemical Physics, 1991, 95, 8561-8567.	3.0	31
29	Investigation of a fatty acid monolayer at the air-water interface using a current-measuring technique. Thin Solid Films, 1989, 178, 67-72.	1.8	30
30	Molecular Orientation of Individual Lu@C <sub>82</sub> Molecules Demonstrated by Scanning Tunneling Microscopy. Journal of Physical Chemistry C, 2010, 114, 14704-14709.	3.1	27
31	Controlled electroplating and electromigration in nickel electrodes for nanogap formation. Nanotechnology, 2010, 21, 445304.	2.6	26
32	Analysis of scanning probe used for simultaneous measurement of tunneling current and surface potential. Journal of Applied Physics, 1999, 86, 7087-7093.	2.5	25
33	Platonic Hexahedron Composed of Six Organic Faces with an Inscribed Au Cluster. Journal of the American Chemical Society, 2012, 134, 816-819.	13.7	25
34	One by one single-electron transport in nanomechanical Coulomb blockade shuttle. Applied Physics Letters, 2007, 91, .	3.3	24
35	Nanoparticle single-electron transistor with metal-bridged top-gate and nanogap electrodes. Applied Physics Letters, 2011, 99, .	3.3	24
36	Ideal Discrete Energy Levels in Synthesized Au Nanoparticles for Chemically Assembled Single-Electron Transistors. ACS Nano, 2012, 6, 9972-9977.	14.6	24

#	Article	IF	CITATIONS
37	Studies on the Dynamic Behavior of Fatty Acid Monolayers at the Air-Water Interface by a Current-Measuring Technique. Japanese Journal of Applied Physics, 1990, 29, 564-568.	1.5	23
38	Au Nanoparticles Chemisorbed by Dithiol Molecules Inserted in Alkanethiol Self-Assembled Monolayers Characterized by Scanning Tunneling Microscopy. Japanese Journal of Applied Physics, 2009, 48, 04C180.	1.5	22
39	Observation of Coulomb staircases of both tunneling current and displacement current in nanomechanical double barrier tunneling structures. Applied Physics Letters, 2002, 81, 544-546.	3.3	21
40	Control of charging energy in chemically assembled nanoparticle single-electron transistors. Nanotechnology, 2015, 26, 045702.	2.6	19
41	Tunneling Current and Surface Potential Simultaneous Measurement Using a Scanning Probe. Japanese Journal of Applied Physics, 1998, 37, 4557-4560.	1.5	18
42	Measurement of semiconductor local carrier concentration from displacement current-voltage curves with a scanning vibrating probe. Physical Review B, 2000, 62, 1971-1977.	3.2	18
43	Revealing the Real Size of a Porphyrin Molecule with Quantum Confinement Probing via Temperature-Dependent Photoluminescence Spectroscopy. Journal of Physical Chemistry A, 2020, 124, 2672-2682.	2.5	18
44	Displacement Current Generated by Photo-Induced Molecular Switching in a Single Monolayer. Japanese Journal of Applied Physics, 1991, 30, 1020-1023.	1.5	17
45	A Smart Food Label Utilizing Roll-to-Roll Gravure Printed NFC Antenna and Thermistor to Replace Existing "Use-By―Date System. IEEE Sensors Journal, 2020, 20, 2106-2116.	4.7	17
46	Investigation of a Langmuir Film Using a Current-Measuring Technique: Influence of the Behavior of Monolayers at the Edge of the LB Trough. Japanese Journal of Applied Physics, 1989, 28, 1922-1925.	1.5	16
47	Interfacial electronic density of states in phthalocyanine derivative Langmuir–Blodgett films determined by surface potential measurement. Journal of Applied Physics, 1999, 86, 3848-3852.	2.5	16
48	Anomalous negative differential conductance in nanomechanical double barrier tunneling structures. Applied Physics Letters, 2005, 87, 163110.	3.3	16
49	Coherent Resonant Electron Tunneling at 9 and 300 K through a 4.5 nm Long, Rigid, Planar Organic Molecular Wire. ACS Omega, 2018, 3, 5125-5130.	3.5	16
50	Reversible Displacement Current Generation Due to Photochromism in a Spread Monolayer: Influence of Molecular Orientation. Japanese Journal of Applied Physics, 1992, 31, 864-867.	1.5	14
51	Maxwell displacementâ€current generation due totransâ€cisphotoisomerization in monolayer Langmuir–Blodgett film. Journal of Applied Physics, 1992, 72, 1637-1641.	2.5	14
52	Polysilane spherulites and their high photoluminescence quantum yields. Journal of Polymer Science Part A, 1997, 35, 427-430.	2.3	14
53	Chemically assembled double-dot single-electron transistor analyzed by the orthodox model considering offset charge. Journal of Applied Physics, 2015, 118, .	2.5	14
54	Polymerization of a divalent/tetravalent metal-storing atom-mimicking dendrimer. Science Advances, 2016, 2, e1601414.	10.3	14

#	Article	IF	CITATIONS
55	Rhombic Coulomb diamonds in a single-electron transistor based on an Au nanoparticle chemically anchored at both ends. Nanoscale, 2016, 8, 4720-4726.	5.6	14
56	Study of the Dynamic Behavior of Stearic Acid Monolayers at the Air-Water Interface in the Range of Low Surface Pressures by a Current-Measuring Technique. Japanese Journal of Applied Physics, 1991, 30, 126-130.	1.5	13
57	Orientational order study of 4-alkyl-4′-cyanobiphenyl Langmuir films by Maxwell displacement current and optical second harmonic generation measurements. Thin Solid Films, 2001, 393, 86-91.	1.8	13
58	Simultaneous Measurements of Drain-to-Source Current and Carrier Injection Properties of Top-Contact Pentacene Thin-Film Transistors. Japanese Journal of Applied Physics, 2007, 46, 390-393.	1.5	13
59	Frequency Dependences of Displacement Current and Channel Current in Pentacene Thin-Film Transistors. Japanese Journal of Applied Physics, 2008, 47, 3167-3169.	1.5	13
60	Characterization of thiol-functionalized oligo(phenylene-ethynylene)-protected Au nanoparticles by scanning tunneling microscopy and spectroscopy. Applied Physics Letters, 2012, 101, 083115.	3.3	13
61	Random telegraph signals by alkanethiol-protected Au nanoparticles in chemically assembled single-electron transistors. Journal of Applied Physics, 2013, 114, .	2.5	13
62	Three-input gate logic circuits on chemically assembled single-electron transistors with organic and inorganic hybrid passivation layers. Science and Technology of Advanced Materials, 2017, 18, 374-380.	6.1	13
63	Single-molecule single-electron transistor (SM-SET) based on π-conjugated quinoidal-fused oligosilole and heteroepitaxial spherical Au/Pt nanogap electrodes. Applied Physics Express, 2019, 12, 125007.	2.4	13
64	Robust Pt-based nanogap electrodes with 10 nm scale ultrafine linewidth. Applied Physics Express, 2019, 12, 025002.	2.4	13
65	Displacement Current Staircase in Mechanical Single-Electron Turnstiles. Japanese Journal of Applied Physics, 2002, 41, 5381-5385.	1.5	12
66	Synthesis and characterization of hollow α-Fe2O3 sub-micron spheres prepared by sol–gel. Hyperfine Interactions, 2011, 202, 131-137.	0.5	12
67	Secondary resonance magnetic force microscopy. Journal of Applied Physics, 2012, 111, 084312.	2.5	12
68	Molecular floating-gate single-electron transistor. Scientific Reports, 2017, 7, 1589.	3.3	12
69	Energy Transfer and Electron Transfer Distances in Heteropolysilane Langmuirâ^'Blodgett Films. Macromolecules, 1996, 29, 4187-4191.	4.8	11
70	Interface trap level in top-contact pentacene thin-film transistors evaluated by displacement current measurement. Organic Electronics, 2010, 11, 594-598.	2.6	11
71	Novel approach for hole-blocking in light-emitting electrochemical cells. Synthetic Metals, 1997, 91, 87-89.	3.9	10
72	Effect of the metal/organic interface phenomena on the current–voltage characteristics of organic single electron tunneling device. Thin Solid Films, 2001, 393, 379-382.	1.8	10

#	Article	IF	CITATIONS
73	Synthesis, Structure, Physical Properties, and Displacement Current Measurement of an n-Type Organic Semiconductor: 2:3,5:6-Bis(1,1-dicyanoethylene-2,2-dithiolate)-quinone. Australian Journal of Chemistry, 2012, 65, 1674.	0.9	10
74	Radio-frequency capacitance spectroscopy of metallic nanoparticles. Scientific Reports, 2015, 5, 10858.	3.3	10
75	Origin of mobility enhancement by chemical treatment of gate-dielectric surface in organic thin-film transistors: Quantitative analyses of various limiting factors in pentacene thin films. Journal of Applied Physics, 2015, 118, .	2.5	10
76	Heteroepitaxial spherical electroless Au-plated Pt-based nanogap electrodes of radius 5 nm and gap separation 0.7 nm. Applied Physics Express, 2019, 12, 125003.	2.4	10
77	20-nm-Nanogap oxygen gas sensor with solution-processed cerium oxide. Sensors and Actuators B: Chemical, 2021, 343, 130098.	7.8	10
78	Molecular switching in phospholipid-azobenzene mixed monolayers by photoisomerization. Thin Solid Films, 1998, 331, 239-247.	1.8	9
79	Interfacial Electrostatic Phenomena in Phthalocyanine Langmuir-Blodgett Films under Photoillumination. Japanese Journal of Applied Physics, 2001, 40, 1315-1321.	1.5	9
80	Room-temperature single molecular memory. Applied Physics Letters, 2012, 100, 053101.	3.3	9
81	Silicon–Nitride-Passivated Bottom-Up Single-Electron Transistors. Japanese Journal of Applied Physics, 2013, 52, 110101.	1.5	9
82	Coulomb blockade and Coulomb staircase behavior observed at room temperature. Materials Research Express, 2017, 4, 024004.	1.6	9
83	Photoisomerization of Azobenzene Dendrimer Monolayer Investigated by Maxwell Displacement Current Technique. Japanese Journal of Applied Physics, 2001, 40, 7085-7090.	1.5	8
84	Analytical Model of Organic Field-Effect Transistor Based on Gradual Channel Approximation with Field-Dependent Mobility. Japanese Journal of Applied Physics, 2006, 45, L27-L29.	1.5	8
85	Stochastic Single-Molecule Conductance Switching of Nitro-Substituted Oligo(phenylene-ethynylene) in Matrix of Low-Density Alkanethiol Self-Assembled Monolayers. Japanese Journal of Applied Physics, 2006, 45, L840-L842.	1.5	8
86	Memory operations in Au nanoparticle single-electron transistors with floating gate electrodes. Applied Physics Letters, 2016, 109, .	3.3	8
87	Thermal oxidation of amorphous germanium thin films on SiO <sub>2</sub> substrates. Semiconductor Science and Technology, 2016, 31, 125017.	2.0	8
88	Enhancement of discrete changes in resistance in engineered VO <sub>2</sub> heterointerface nanowall wire. Applied Physics Express, 2017, 10, 115001.	2.4	8
89	An Electroactive Binder in the Formulation of IGZO Ink to Print an IGZOâ€Based Rectifier for Harvesting Direct Current (DC) Power from the Near Field Communication (NFC) Signal of a Smartphone. Advanced Electronic Materials, 2018, 4, 1800078.	5.1	8
90	Detection of optical molecular switching in monolayers by displacement current measurement. Thin Solid Films, 1992, 210-211, 82-85.	1.8	7

#	Article	IF	CITATIONS
91	Generation of the displacement current by the transformation of J-aggregates in spreading monolayers of squarylium dye. Chemical Physics Letters, 1992, 195, 45-49.	2.6	7
92	Dielectric Relaxation Phenomena of a Liquid Crystal Monolayer at the Air-Water Interface. Japanese Journal of Applied Physics, 1997, 36, 5237-5241.	1.5	7
93	The waveform separation of displacement current and tunneling current using a scanning vibrating probe. Thin Solid Films, 2001, 393, 204-209.	1.8	7
94	Space charge effect and the step voltages in metal/polyimide/rhodamine–dendorimer/polyimide/metal junctions. Journal of Applied Physics, 2001, 90, 1368-1375.	2.5	7
95	TiO[sub 2] Composites for Efficient Poly(3-thiophene acetic acid) Sensitized Solar Cells. Journal of the Electrochemical Society, 2011, 158, B106.	2.9	7
96	Impact of Orbital Hybridization at Molecule–Metal Interface on Carrier Dynamics. Journal of Physical Chemistry C, 2019, 123, 25877-25882.	3.1	7
97	Resistive Switching Effects in Metallic Nanogap Electrode Fabricated by Electroless Gold Plating. Applied Physics Express, 2012, 5, 085201.	2.4	7
98	Detection of electron transfer between single monolayers by a Maxwell-displacement-current measuring technique. Physical Review B, 1992, 46, 10479-10482.	3.2	6
99	Oxygen-crosslinked polysilane: the new class of Si-related material for electroluminescent devices. Polymers for Advanced Technologies, 1997, 8, 465-470.	3.2	6
100	Integration of colloidal silicon nanocrystals on metal electrodes in single-electron transistor. Applied Physics Letters, 2016, 109, .	3.3	6
101	Formation of L1 <sub>0</sub> -ordered CoPt during interdiffusion of electron-beam-deposited Pt/Co bilayer thin films on Si/SiO <sub>2</sub> substrates by rapid thermal annealing. Materials Research Express, 2020, 7, 066101.	1.6	6
102	Thermodynamic Picture of Phase Segregation during the Formation of Bicontinuous Concentric Lamellar ( <i>bcl</i> ) Silica. Langmuir, 2022, 38, 1368-1379.	3.5	6
103	Detection of Electron Transfer in Multilayer Systems by a Displacement Current-Measuring Technique. Japanese Journal of Applied Physics, 1992, 31, 2140-2144.	1.5	5
104	A living monolayer of lipid showing well-regulated displacement-current generation. Thin Solid Films, 1992, 210-211, 86-88.	1.8	5
105	Space charge distribution of organic-molecular-beam-deposited titanylphthalocyanine films on metal electrodes. Journal of Applied Physics, 1999, 86, 3229-3233.	2.5	5
106	Scanning Lorentz force microscopy. Applied Physics Letters, 2002, 81, 2872-2874.	3.3	5
107	Observation of Displacement Current Staircase and Negative Differential Resistance in Nanomechanical Double-Barrier Tunneling Structures with Scanning Vibrating Probe. Japanese Journal of Applied Physics, 2003, 42, 2458-2461.	1.5	5
108	Observation of Current Modulation through Self-Assembled Monolayer Molecule in Transistor Structure. Japanese Journal of Applied Physics, 2004, 43, L337-L339.	1.5	5

#	Article	IF	CITATIONS
109	Attaching Thiolated Superconductor Grains on Gold Surfaces for Nanoelectronics Applications. Japanese Journal of Applied Physics, 2010, 49, 093102.	1.5	5
110	Surface Potential of 1,10-Decanedithiol Molecules Inserted into Octanethiol Self-Assembled Monolayers on Au(111). Journal of Physical Chemistry C, 2010, 114, 8120-8125.	3.1	5
111	Interdiffusion during heteroepitaxial Au growth on Pd thin films by electroless Au plating (ELGP) at room temperature. Applied Physics Express, 2020, 13, 015006.	2.4	5
112	Towards single electron transistor-based photon detection with microplasma-enabled graphene quantum dots. Nanotechnology, 2021, 32, 50LT01.	2.6	5
113	Ti underlayer effect on the ordering of CoPt in (Co/Pt) <sub>4</sub> multilayer thin films on Si/SiO <sub>2</sub> substrates. Japanese Journal of Applied Physics, 2020, 59, 075504.	1.5	5
114	Anomalous Transition in Charge Transport Behavior of Polysilane. Japanese Journal of Applied Physics, 1995, 34, 3820-3824.	1.5	4
115	Determination of the Piezoelectric Coefficient of Monolayers on Water Surface by Maxwell-Displacement-Current Measurement. Japanese Journal of Applied Physics, 1998, 37, 215-216.	1.5	4
116	Determination of Dielectric Relaxation Time of Langmuir-Films by a Whole-Curve Method Using the Maxwell Displacement Current. Japanese Journal of Applied Physics, 1998, 37, 5655-5658.	1.5	4
117	Cantilever Resonance Detected by Tunneling Current under Application of RF Signal. Japanese Journal of Applied Physics, 2007, 46, 3152-3154.	1.5	4
118	Aging effect in CaLaBa{Cu1 â^' xFex}3O7 â^' δ with 0 ≤ ≤0.07 studied by Mössbauer s Interactions, 2011, 203, 119-124.	pectrosco 0.5	ppy <mark>.</mark> Hyperfine
119	The Irreversibility Line and Curie-Weiss Temperature of the Superconductor LaCaBaCu3-X(BO3)X with x= 0.2 and 0.3. Physics Procedia, 2012, 36, 354-359.	1.2	4
120	Coulomb blockade behaviors in individual Au nanoparticles as observed through noncontact atomic force spectroscopy at room temperature. Nanotechnology, 2012, 23, 185704.	2.6	4
121	Characterization of copper microelectrodes, following a homemade lithography, technique, and gold electroless deposition. Revista Materia, 2016, 21, 252-259.	0.2	4
122	Solutionâ€Processed Silicane Fieldâ€Effect Transistor: Operation Due to Stacking Defects on the Channel. Advanced Functional Materials, 2020, 30, 1908746.	14.9	4
123	Rollâ€ŧoâ€Roll Gravureâ€₽rinted Carbon Nanotubeâ€based Transistor Arrays for a Digital Column Chromatograph. Advanced Materials Technologies, 0, , 2101243.	5.8	4
124	Detection of the reorganization of monolayers at the air-water interface by displacement current measurement. Thin Solid Films, 1992, 210-211, 101-104.	1.8	3
125	Interfacial electrostatic phenomena in phthalocyanine Langmuir–Blodgett films. Colloids and Surfaces A: Physicochemical and Engineering Aspects, 2002, 198-200, 729-734.	4.7	3
126	Individual transport of electrons through a chemisorbed Au nanodot in Coulomb blockade electron shuttles. Journal of Applied Physics, 2011, 109, .	2.5	3

#	Article	IF	CITATIONS
127	Single-Electron Transistor made by Au Nanoparticles and Nanogap Electrodes. Journal of the Vacuum Society of Japan, 2012, 55, 328-332.	0.3	3
128	Reorientation Response of Magnetic Microspheres Attached to Gold Electrodes Under an Applied Magnetic Field. Brazilian Journal of Physics, 2013, 43, 209-213.	1.4	3
129	Orientational Transition of P-pentyl-p'-cyano-biphenyls Triggered by Conformational Change of Surface Azobenzene Monolayer. Japanese Journal of Applied Physics, 1999, 38, 5984-5990.	1.5	2
130	Analysis of the Dielectric Relaxation Property of Phospholipid Monolayers by Maxwell Displacement Current Measurement. Journal of Colloid and Interface Science, 1999, 218, 118-121.	9.4	2
131	Interaction Control Between Endohedral Metallofullerene and Metal Substrate by Introducing Alkanethiol Self-Assembled Monolayer. Journal of Nanoscience and Nanotechnology, 2006, 6, 3460-3463.	0.9	2
132	Quantum Chemical Studies on Electron-Accepting Overcrowded Ethylene with a Polarizable Skeleton. Journal of Physical Chemistry A, 2017, 121, 7797-7806.	2.5	2
133	Large coercivity of 13 kOe in L1 <sub>0</sub> -ordered CoPt on Si/SiO <sub>2</sub> substrates by hydrogen annealing. Japanese Journal of Applied Physics, 2022, 61, 065002.	1.5	2
134	Analysis of dielectric relaxation phenomena of monolayer films by monolayer compression. Thin Solid Films, 1998, 327-329, 228-231.	1.8	1
135	Investigation of dielectric relaxation phenomena in liquid crystal monolayer at the air–water interface. Thin Solid Films, 1998, 327-329, 232-235.	1.8	1
136	Simultaneous observation of magnetic domain structure and topography of Fe70Co30 using scanning Lorentz force microscopy. Applied Physics Letters, 2007, 90, 053110.	3.3	1
137	A Study of the Behavior of SE and BSE in UltraLow Landing Voltage Condition. Microscopy and Microanalysis, 2009, 15, 662-663.	0.4	1
138	Mössbauer study of contaminated soils by industrial activity in Paramonga city, Region Lima Provinces, Peru. Hyperfine Interactions, 2012, 211, 147-152.	0.5	1
139	Epitaxial growth of YBa <sub>2</sub> Cu <sub>3</sub> 0 <sub>7â~îí</sub> films on SrTiO <sub>3</sub> (100) by direct solution precursor deposition. Journal of Physics: Conference Series, 2014, 507, 012005.	0.4	1
140	Determination of Surface Space Charge Density on Semiconductor from Displacement Current-Voltage Curve using a Scanning Vibrating Probe. Materials Research Society Symposia Proceedings, 2001, 699, 431.	0.1	0
141	Development of Scanning Displacement Current Microscope. Molecular Crystals and Liquid Crystals, 2001, 370, 297-300.	0.3	0
142	Small Au/SAM/Au junctions by EB lithography. , 2003, 4999, 307.		0
143	Detection of One-Angstrom Deformation of Au(111)/Mica Cantilever due to Thermal Expansion under the Application of Resonant RF Signal by Tunneling Current. Japanese Journal of Applied Physics, 2007, 46, L920-L922.	1.5	0
144	Single-electron transistors fabricated by electroless plated nanogap electrodes and chemisorbed Au nanoparticles. , 2010, , .		0

#	Article	IF	CITATIONS
145	Ripple-Free Graphene Sheets on Alkanethiol Self-Assembled Monolayers Provided from Unzipped Multi-Walled Carbon Nanotubes. Journal of Nanoscience and Nanotechnology, 2015, 15, 1203-1208.	0.9	0
146	The APEX Review—a new article type for APEX. Applied Physics Express, 2018, 11, 030001.	2.4	0
147	Suppression Mechanisms of the Solid-Electrolyte Interface Formation at the Triple-Phase Interfaces in Thin-Film Li-Ion Batteries. ACS Applied Materials & amp; Interfaces, 2021, 13, 34027-34032.	8.0	0
148	Verification of Au Nanodot Size Dependence on Coulomb Step Width by Non-contact Atomic-force Spectroscopy. IEICE Transactions on Electronics, 2006, E89-C, 1755-1757.	0.6	0
149	Special Section on Towards the Realization of Organic Molecular Electronics. IEICE Transactions on Electronics, 2006, E89-C, 1725-1726.	0.6	0
150	STM Characterization of Ï $\in$ -Electron Systems. , 2015, , 621-634.		0